Dyes and Pigments **11** (1989) 213–232

Fluorescence Quenching Studies of the Self-Association in Water of Fluorescent Surfactants. Alkaryl-2-pyrazolines and Alkyl-7-hydroxycoumarins

L. E. Aicolina, I. H. Leaver* & I. W. Stapleton

CSIRO, Division of Wool Technology, 343 Royal Parade, Parkville 3052, Australia

(Received 1 September 1988; accepted 12 October 1988)

ABSTRACT

This paper reports on the spectral properties of a range of alkaryl-2-pyrazolines and 3-alkyl-7-hydroxycoumarins containing n-*alkyl substituents of varying chain length and examines the self-association behaviour of these compounds in water using a variety of spectroscopic techniques. For the higher members of each series, plots of the fluorescence quantum yield vs the solute concentration showed a sharp decrease in fluorescence yield at a well-defined concentration, in contrast to the smoothly decreasing curve that was characteristic of the lower members of the series. The kinetics of the fluorescence quenching were consistent with the formation of micelles from the surfactant monomers. Solubilization of two lipid probes, Nile Red and NBD-dioctylamine, by micelles of long-chain 3-alkyl-7-hydroxycoumarin sulphonates was accompanied by a strong enhancement of their fluorescence; the same probes showed little affinity for binding to micelles of alkaryl-2-pyrazoline sulphonates or quaternary ammonium pyrazoline derivatives. The micellar aggregation number of the highest member of the coumarin series was determined from fluorescence quenching experiments employing tris (2,2′-bipyridine)ruthenium (II) dichloride and 9-methylanthracene.*

1 INTRODUCTION

Fluorescence techniques have been employed widely in the study of micelle structure and dynamics.[1–3] The fluorescence probe approach utilizes

* To whom correspondence should be addressed.

Dyes and Pigments 0143-7208/89/$03·50

changes in some readily observable property of the probe molecule (such as its excitation or emission spectrum, decay time or quantum yield of emission) to report on the local micellar structure in the vicinity of the probe. If the surfactant molecule has an environmentally sensitive fluorescent moiety as an integral part of the structure, then the process of micellization may be revealed[2,4,5] through changes in the intrinsic emission properties of the surfactant itself, without the need for introducing an extrinsic probe.

Recently, a range of fluorescent alkaryl-2-pyrazoline and 3-alkyl-7-hydroxycoumarin derivatives carrying *n*-alkyl substituents of varying chain length have been synthesized[6,7] for use as microscopic tracers, in order to examine the pathways for the diffusion of surfactants into the wool fibre. Depending on its amphiphilic character and the conditions under which it is applied, the surfactant may be deposited at the fibre surface or in the intercellular and cell remnant regions within the fibre.[6,7]

The interpretation of results arising from the use of such probes as models for micellar systems requires a detailed knowledge of the spectral properties of the probe molecules and the manner in which their emission characteristics change in response to changes in the microenvironment. It was the purpose of this research to characterize the spectral properties of a series of anionic alkaryl-2-pyrazoline sulphonates (designated PS-*n*, where *n* is the number of carbon atoms in the alkyl side-chain) and 3-alkyl-7-hydroxycoumarin sulphonates (CS-*n*) and cationic quaternary ammonium

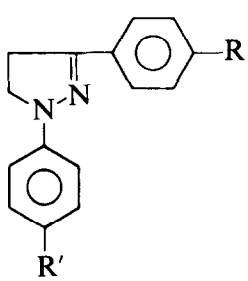

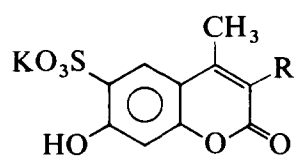

	R	R′
PS-0	H	$SO_3^-Na^+$
PS-3	$CH_3(CH_2)_2$—	—$SO_3^-NH_4^+$
PS-6	$CH_3(CH_2)_5$—	—$SO_3^-NH_4^+$
PS-9	$CH_3(CH_2)_8$—	—$SO_3^-NH_4^+$

	R
CS-0	H
CS-4	$CH_3(CH_2)_3$—
CS-6	$CH_3(CH_2)_5$—
CS-8	$CH_3(CH_2)_7$—
CS-10	$CH_3(CH_2)_9$—

PN-0	H	—$CH_2N^+(CH_3)_3.CH_3SO_4^-$
PN-3	$CH_3(CH_2)_2$—	—$CH_2N^+(CH_3)_3.CH_3SO_4^-$
PN-6	$CH_3(CH_2)_5$—	—$CH_2N^+(CH_3)_3.CH_3SO_4^-$
PN-9	$CH_3(CH_2)_8$—	—$CH_2N^+(CH_3)_3.CH_3SO_4^-$

alkaryl-2-pyrazolines (PN-*n*) in aqueous and micellar environments, and to investigate the self-association behaviour of these amphiphiles using fluorescence probing methods.

2 EXPERIMENTAL

2.1 Pyrazoline synthesis

The members of the cationic pyrazoline series were prepared by the normal condensation and ring-closure reaction involving a *p*-alkylpropiophenone and *p*-hydrazino-*N*,*N*-dimethylbenzylamine. The pendant *tert.* amino group was subsequently quaternized with dimethylsulphate.

The following preparation of 1-([4′-trimethylaminomethyl]phenyl)-3-(4′-nonylphenyl)-2-pyrazoline-ium methosulphate (PN-9) is typical for all members of the series.

(a) *p*-Hydrazino-*N*,*N*-dimethylbenzylamine was prepared from *p*-aminodimethylbenzylamine[8] by a diazotization and sulphite reduction procedure which has previously been described[9] for the preparation of phenylhydrazine. Because the product could not be isolated as a mineral acid salt, the free base was liberated by the addition of 10M NaOH to the cooled (5–10°C) solution at the conclusion of the reduction. The aminohydrazine was extracted with several portions of ether which were combined, dried over Na_2SO_4 and the solvent removed in a rotary evaporator at a bath temperature not exeeding 20°C. This precaution is necessary as the oily product proved to be unstable at elevated temperatures. The NH region of the IR spectrum was in accord with the replacement of a primary amino group (ν_{NH} 3220, 3350 cm^{-1}) by a hydrazino group (ν_{NH} 3320 cm^{-1}). The product was stored at −10°C and used directly in the next step.

(b) The above crude aminohydrazine (0·6 g) and 4-*n*-nonyl-*β*-dimethylaminopropiophenone hydrochloride[6] (1·0 g) were dissolved in warm ethanol (8 ml). The resulting solution was treated with 2M NaOH (1·5 ml) and heated under reflux for 4 h. The hydrochloride of the resulting *tert*-aminopyrazoline was isolated by adding conc. HCl (2 ml) to the cooled solution and filtering off the salt after 4 h standing at 0°C. The crystalline product (0·54 g) after crystallization from methanol–ether gave m.p. 218–219°C. (Found: N, 9·2; Cl, 7·5%. Calc. for $C_{27}H_{40}ClN_3$: N, 9·5; Cl, 8·0%.) Other dimethylaminomethylhydrochloride salts of the series gave mp. 219–220°C (R = H), 223–225°C (R = C_3H_7) and 224–225°C (R = C_6H_{13}).

To form the quaternary salt, the free base was first isolated by treating a warm aqueous solution of the *tert*-amino hydrochloride with sodium

carbonate (10%) and extraction with ethyl acetate. The extract was dried over Na_2SO_4 and treated with dimethyl sulphate (0·3 ml). After keeping the solution at 50°C for 1 h, the solid methosulphate salt was filtered off, washed with ethyl acetate and crystallized from methyl cellosolve–ether as yellow needles (0·7 g); no definite mp (softens at 90°C). (Found: N, 7·6; S, 6·2%. Calc. for $C_{29}H_{45}N_3O_4S$: N, 7·9; S, 6·0%.) The mps of the other quaternary methosulphate salts of the series were found to be: 152–154°C (ethanol–cyclohexane), 137–138°C (methanol–ether) and 122–123°C (propanol–cyclohexane) for PN-0, PN-3 and PN-6 respectively.

The syntheses of the anionic pyrazoline sulphonates (PS-*n*) and the 3-alkyl-7-hydroxycoumarin sulphonates (CS-*n*) are described elsewhere.[6]

2.2 Materials

Sodium dodecyl sulphate (BDH, specially pure), Triton X-100 (BDH, 100% active constituent) and cetyltrimethylammonium chloride (TCI, >95% purity) were used without further purification. The fluorescent probes Nile Red, NBD-dioctylamine and 9-methylanthracene were purchased from Molecular Probes, Inc. and tris-(2,2′-bipyridine)-ruthenium (II) dichloride ($Ru(bipy)_3^{2+}$) from Sigma Chemical Company. Quinine sulphate dihydrate (BDH) was purified by recrystallization twice from water.

2.3 Spectral measurements

Absorption spectra were recorded on a Shimadzu UV-265 spectrophotometer and corrected fluorescence spectra were recorded on a Hitachi F-4000 spectrofluorimeter which has built-in data processing functions for spectral correction. Fluorescence quantum yields (ϕ) were determined relative to that of quinine sulphate in 0·5M H_2SO_4 ($\phi = 0{\cdot}546$).[10] Measurements on dilute samples (10^{-6} to 5×10^{-5} M) were made using a conventional right-angle geometry for excitation and emission with excitation at or near the wavelength of maximum absorption. Fluorescence intensities were recorded for air-saturated aqueous solutions of the compounds in cuvettes having an optical pathlength of 10 or 3·2 mm. Measurements on concentrated samples (5×10^{-5} to 10^{-2} M) were obtained on a Perkin–Elmer MPF-3L spectrofluorimeter (equipped with spectral correction facilities) using a front-surface sample-holder having an optical geometry of normal incidence and near-normal viewing of the emitted fluorescence.[11] The procedures for correcting the measured intensities for absorption and inner filter effects are described in Section 3.2.

For the determination of critical micelle concentrations using the

fluorescent probe Nile Red, aliquots (10 μl) of the stock solution of the probe (5×10^{-4} M) in ethanol were transferred by micropipette to aqueous solutions (1 ml) containing known amounts of the fluorescent surfactant. Fluorescence intensities were measured by exciting the probe fluorescence at 540 nm and monitoring the emission at 640 nm.

The critical micelle concentration and mean micellar aggregation number of the coumarin CS-10 were determined by the fluorescence quenching method of Turro & Yekta,[12] which employs the cation $Ru(bipy)_3^{2+}$ as donor and 9-methylanthracene as quencher. For experiments performed at fixed quencher concentration, a series of solutions (1 ml) containing known amounts of the coumarin and $Ru(bipy)_3^{2+}$ (10^{-5} M) together with a measured quantity of 9-methylanthracene (5 μl of a 4×10^{-3} M stock solution in ethanol) was prepared for analysis. Fluorescence intensities were measured using excitation and emission wavelengths of 450 and 640 nm, respectively, with a red filter (Hitachi R-63) placed in the emission beam to minimize errors due to light scattering. For experiments performed at fixed coumarin concentration, aliquots of the 9-methylanthracene stock solution were added, in 5-μl increments, to an aqueous solution of the coumarin (4×10^{-3} M) containing $Ru(bipy)_3^{2+}$, and the fluorescence intensities measured as described above. The sample temperature for these experiments was 50°C.

3 RESULTS AND DISCUSSION

3.1 Spectral properties

In the polycrystalline form, the alkaryl-2-pyrazolines and alkyl-7-hydroxycoumarins all fluoresced intensely under UV excitation. Within each series of compounds the fluorescence emission systematically changed in colour from blue to yellow and then to blue again as the length of the alkyl side-chain increased. The polymorphism of the long-chain amphiphiles is very rich, as shown by the variety of crystal forms of varying shape and colour seen when freshly grown crystals (obtained by slow evaporation to dryness of an ethanol–water solution) were viewed in the fluorescence microscope.

The sensitivity of the fluorescence emission spectra of the polycrystalline surfactants to changes in molecular structure is illustrated in Fig. 1. The introduction of a side-chain containing between three and six carbon atoms produced red shifts of up to 30, 59 and 108 nm in the emission maxima of the pyrazoline sulphonates, quaternary ammonium pyrazolines and coumarin sulphonates, respectively. Derivatives in which the alkyl substituent is

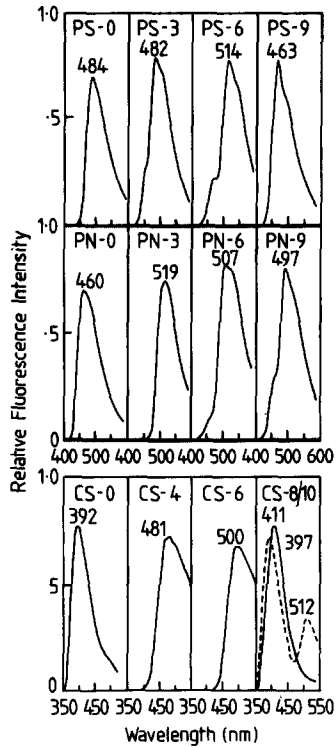

Fig. 1. Corrected fluorescence emission spectra of alkaryl-2-pyrazoline sulphonates (PS-*n*), quaternary ammonium alkaryl-2-pyrazolines (PN-*n*) and alkyl-7-hydroxycoumarins (CS-*n*) in the polycrystalline form. The spectrum of CS-10 is shown by the broken curve.

greater than six carbon atoms in length showed a reversal of this trend, the effect being more pronounced in the anionic than in the cationic series. The polymorphism of the higher members of each series is evident from the structured appearance of their emission spectra.

The emission characteristics of the fluorescent surfactants showed much less diversity in aqueous solution than in the polycrystalline form. Table 1 summarizes the spectral properties of the three series of compounds in water and in various aqueous micellar systems.

An increase in the size of the alkyl side-chain affected only slightly the absorption and emission maxima and fluorescence quantum yields of the fluorophors in water. The fluorescence of members of both series of pyrazolines (PS-*n* and PN-*n*) was enhanced by the presence of surfactants (above their critical micelle concentrations), indicating some degree of penetration of these molecules into the surfactant micelle. This effect was most pronounced for solutions of the pyrazoline sulphonates containing the nonionic surfactant, Triton X-100. Although the attachment of a

TABLE 1
Absorption and Fluorescence Maxima and Fluorescence Quantum Yields in Water and Various Amphiphilic Media

Compound	λ_{max} (*abs*) (*nm*)	λ_{max} (*em*) (*nm*)	*Fluorescence quantum yield*			
			Water (ϕ_0)	*SDS* (*0·05* M)	*CTAC* (*0·05* M)	*Triton X-100* (*0·05* M)
PS-0	356	485	0·32	0·42	0·79	0·89
PS-3	359	485	0·39	0·55	0·80	0·95
PS-6	357	482	0·40	0·59	0·77	0·77
PS-9	358	486	0·35	0·59	0·68	0·98
PN-0	355	487	0·35	0·71	0·43	0·66
PN-3	359	486	0·44	0·68	0·64	0·68
PN-6	357	484	0·45	0·64	0·66	0·68
PN-9	357	484	0·36	0·63	0·68	0·68
CS-0	318	473	0·61	0·66	0·39	0·40
CS-4	321	471	0·62	0·54	0·58	0·30
CS-6	320	474	0·60	0·46	0·61	0·26
CS-8	321	473	0·59	0·52	0·76	0·27
CS-10	321	474	0·60	0·48	0·80	0·32

hydrophobic side-chain to the pyrazoline ring system might be expected to make the association between solute and micelle more favourable, and thereby enhance the fluorescence even further, the fluorescence quantum yields in micellar solutions were generally insensitive to changes in the length of the alkyl group.

The fluorescence quantum yields of the coumarins (CS-*n*) in water were generally lowered upon addition of a surfactant (see Table 1). The interpretation of these changes is complicated, however, by the sensitivity of the coumarin fluorophor to the hydrogen bonding properties of the environment.[13,14] Interestingly, micellar solutions of the long-chain coumarins exhibited very broad emission spectra comprising overlapping bands due to both the acidic and basic forms of the solute, and a proper interpretation of the spectral changes would have to take into account both the ground and excited state protolytic equilibria in these systems. The photophysical properties of coumarin dyes in both hydrogen bonding and amphiphilic media have been discussed elsewhere.[13,14]

3.2 Concentration quenching of fluorescence

Relationship between fluorescence intensity and concentration
The emission properties of fluorescent surfactants in solution might be expected to show a strong dependence upon concentration if, like ordinary

surfactants, they spontaneously form micellar aggregates at a particular concentration. Before investigating the self-association behaviour of the pyrazolines and coumarins, steps were taken to develop a reliable method that would allow the fluorescence quantum yields of these strongly absorbing fluorophors to be determined over a wide range of concentrations (10^{-5}–10^{-2} M).

For fluorophor concentrations below 5×10^{-5} M, fluorescence quantum yields were determined using the usual right-angle geometry for excitation and emission. The variation of fluorescence intensity as a function of the solution absorbance (A) at fixed excitation wavelength is given by the equation:[15]

$$\frac{I(A)}{I_{max}} = \frac{[10^{-Ax/l} - 10^{-A(1-x)/l}]}{N_{max}(x/l)} \tag{1}$$

where x/l is the fraction of the cell length (l) at each end of the cell from which no emission is collected ($[1 - 2x/l]$ being the central fraction of the cell length from which emission is collected). $I(A)$ has been normalized to its maximum value, $N_{max}(x/l)$.

Values for the fractional cell length (x/l) were determined by measuring the variation of fluorescence intensity as a function of solution absorbance for a series of quinine sulphate solutions having absorbances (per cm) in the range 0–1, and then fitting the fluorescence data (using an iterative least squares procedure) to the function:

$$I(A) = k[10^{-Ax/l} - 10^{-A(1-x)/l}] \tag{2}$$

where k is an arbitrary scaling factor. The best fit between the theoretical function and the experimental data yielded values of 0·277 and 0·190 for the fractional cell lengths corresponding to a 1 cm pathlength in the Hitachi F-4000 and MPF-3L spectrofluorimeters, respectively. The normalized function (eqn (1) with $x/l = 0{\cdot}277$) and the appropriately scaled fluorescence intensities (filled symbols) are shown in Fig. 2. Fluorescence quantum yields (ϕ) of the pyrazolines and coumarins were determined relative to the value (ϕ_0) for an infinitely dilute solution of the fluorophor after division of the measured fluorescence intensities by the correction factor given by eqn (1).

For fluorophor concentrations greater than 5×10^{-5} M, a frontal geometry[11] for excitation and emission was employed in order to minimize errors due to inner filter and reabsorption effects. An optical pathlength of 2 mm was employed for these measurements. The measured fluorescence intensities were corrected for the fraction of light absorbed by the sample using the relation:

$$I(A)/I_{max} = [1 - 10^{-A}] \tag{3}$$

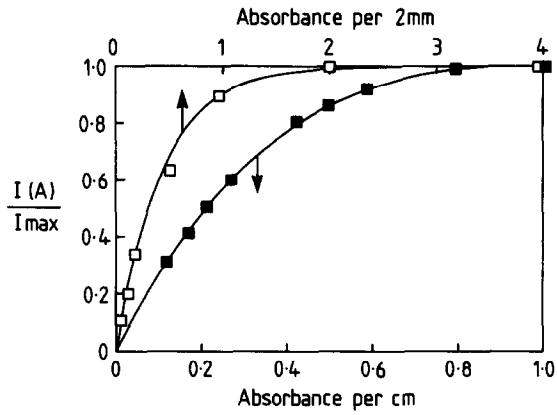

Fig. 2. Dependence of fluorescence intensity upon the absorbance (A) of quinine sulphate solutions measured using (a) a right-angle geometry (■) and (b) a frontal geometry (□) for excitation and emission. The curves show the theoretical relationships appropriate to right-angle and frontal geometries given by eqns (1) and (3), respectively (see text for details). The curve based on eqn (1) was calculated using a value of 0·277 for the fractional cell length (x/l).

The applicability of eqn (3) was checked by determining the variation of fluorescence intensity as a function of fluorophor concentration for a series of quinine sulphate solutions having absorbances (per 2 mm) in the range 0·05–4. The normalized correction function (eqn (3)) and the appropriately scaled fluorescence intensities (open symbols) are shown in Fig. 2. The deviation between the measured and calculated intensities was $<3\%$ over the entire concentration range studied. The maximum fluorescence reading remained constant for quinine sulphate concentrations up to 4×10^{-3} M (absorbance per 2 mm $\sim$ 8), and hence we conclude that errors arising from concentration quenching and reabsorption effects were negligible. Fluorescence quantum yields were determined in the manner described above using eqn (3) to correct for the effects of light absorption.

Self-quenching of fluorescence

The pyrazoline sulphonates all showed some degree of fluorescence quenching in water at high solute concentrations. The dependence of their fluorescence quantum yields (measured relative to the value (ϕ_0) in dilute solution) upon concentration is shown in Fig. 3. For the lower members (PS-0 and PS-3) of this series the fluorescence quenching was quite small and may simply stem from self-absorption of part of the emitted fluorescence by other molecules of the surfactant. The effect of self-absorption is most noticeable in concentrated solution. For the higher members of the series, on the other hand, there was a sharp decrease in the fluorescence quantum yield at relatively low, but well-defined solute concentrations at which inner filter

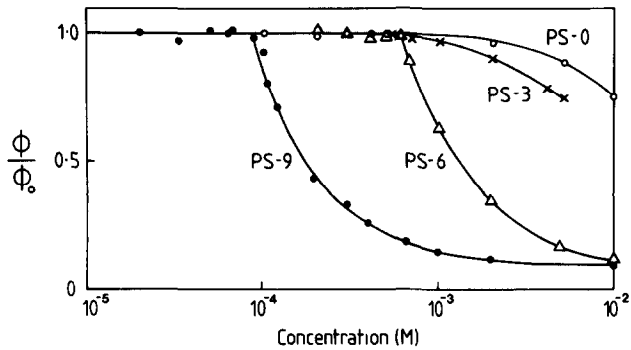

Fig. 3. Dependence of the fluorescence quantum yields of alkaryl-2-pyrazoline sulphonates upon concentration at 25°C in water.

and reabsorption effects are negligible. The discontinuity occurred at a concentration around 6×10^{-4} M and 9×10^{-5} M for the hexyl- and nonyl-substituted pyrazoline sulphonates, respectively.

In contrast to the strong fluorescence quenching shown by the long-chain anionic pyrazolines, the fluorescence quantum yields of the homologous quaternary ammonium compounds (PN-6 and PN-9) were affected only slightly by an increase in solute concentration. The plot of ϕ/ϕ_0 vs concentration for PN-6 showed a small but discernible break at a concentration around 4×10^{-4} M (Fig. 4(a)). The corresponding plot (not shown) for PN-9 showed no evidence of a discontinuity. At high solute concentrations, the fluorescence of the smaller homologues decreased smoothly with increasing concentration, similar in behaviour to the lower members of the pyrazoline sulphonate series.

The fluorescence behaviour of the anionic coumarins paralleled that of the anionic pyrazolines. The ϕ/ϕ_0 vs concentration plots for the two highest members, CS-8 and CS-10, showed strong fluorescence quenching at concentrations greater than 2×10^{-3} M and 10^{-3} M, respectively (see Fig. 4(b)), whereas the plots for the lower members of the series showed only a small, smooth decrease in fluorescence quantum yield in the high concentration region.

Analysis of fluorescence quenching

An abrupt change in the fluorescence characteristics of an amphiphilic fluorophor at a particular concentration is indicative of micellization, the break in the curve being evidence of the formation, at that point, of micelles from unassociated molecules of the fluorophor. By analogy with other micelle-forming systems,[16] we assume that the concentration of the surfactant remains constant once the critical micelle concentration (CMC) is

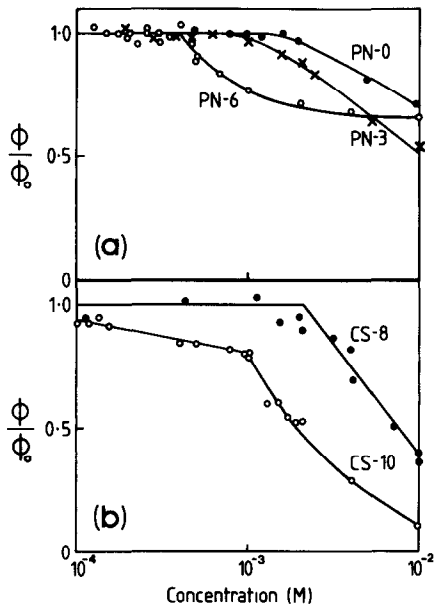

Fig. 4. Dependence of the fluorescence quantum yields of quaternary ammonium alkaryl-2-pyrazolines (a) and 3-alkyl-7-hydroxycoumarin sulphonates (b) upon concentration at 25 and 46°C, respectively, in water.

reached. For concentrations above the CMC, the dependence of the measured fluorescence quantum yield (ϕ) upon the total amphiphile concentration (c) can then be expressed in terms of the fractional absorbances of the unassociated and associated species in the solution, according to the expression:

$$\phi = \frac{\text{CMC} \times \varepsilon_0 \times \phi_0 + (c - \text{CMC}) \times \varepsilon_m \times \phi_m}{\text{CMC} \times \varepsilon_0 + (c - \text{CMC}) \times \varepsilon_m} \tag{4}$$

where ϕ_0, ϕ_m are the fluorescence quantum yields of the free and micellar forms of the surfactant and ε_0, ε_m are the respective absorption coefficients at the wavelength of excitation of the fluorescence. For concentrations below the CMC, the fluorescence arises solely from molecules in the unassociated form, in which case ϕ is equal to ϕ_0.

A simplified form of eqn (4) can be used to analyse systems in which the associated and unassociated species have the same absorption properties. This was shown to be the case for the fluorophors used in this work. Although the fluorescence emission spectra of the pyrazolines and coumarins generally showed a small red shift of the emission maximum at high amphiphile concentrations (0·005–0·01 M), neither the absorption spectra nor the absorption coefficients were significantly altered by a change

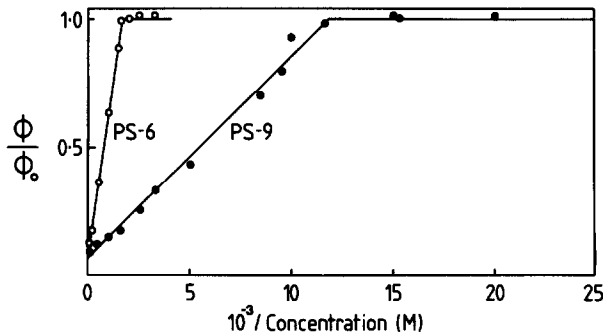

Fig. 5. Dependence of the fluorescence quantum yields of PS-6 and PS-9 upon solute concentration, plotted according to eqn (5). The solid lines represent the lines of best fit.

in concentration. Equation (4) can therefore be simplified to give, after rearrangement, the following expression for the concentration dependence of the fluorescence quantum yield (above the CMC):

$$\frac{\phi}{\phi_0} = \frac{\text{CMC}}{c} \times \left(1 - \frac{\phi_m}{\phi_0}\right) + \frac{\phi_m}{\phi_0} \tag{5}$$

Figure 5 shows the fluorescence quenching data obtained with the long-chain pyrazoline sulphonates (PS-6 and PS-9), replotted according to eqn (5). Above the CMC there is a linear relationship between ϕ/ϕ_0 and the inverse of the amphiphile concentration which allows determination of both the CMC and the fluorescence quantum yield (ϕ_m) of each compound in the micellar form. The CMC values thus obtained from the intercept of the lines of best fit above and below the CMC, together with the calculated micellar fluorescence quantum yields (ϕ_m), are given in Table 2.

The CMCs of the pyrazoline sulphonates are much lower than the values (typically 0·01–0·1 M) for straight-chain anionic surfactants (*n*-alkyl sulphates, *n*-alkane sulphonates) or *p*–*n*-alkylbenzene sulphonates that have a similar number of carbon atoms in the alkyl side-chain. The CMC of PS-6 is close to that of sodium hexadecyl-1-sulphonate (CMC = 7×10^{-4} M),[16] from which we infer that the diphenyl-2-pyrazolyl ring system has an effective length of about 10 carbon atoms in a straight carbon chain. This result seems quite reasonable, given that each phenyl group probably has an effective length of about 3·5 carbon atoms.[16] The presence of three additional methylene groups in the side-chain of PS-9 lowers the CMC by a factor of about seven, which is close to the value ($\sim 2^3 = 8$) predicted from the empirical relationship[16] between the CMC and the number of carbon atoms in the hydrocarbon chain of straight-chain anionic surfactants.

Results obtained from the analysis of the fluorescence quenching data for the cationic pyrazoline (PN-6) and the anionic coumarins (CS-8 and CS-10)

TABLE 2
Micellar Parameters for Fluorescent Surfactants Obtained from Fluorescence Quenching Measurements

Compound	*Temp.* (°C)	*CMC* (M)	ϕ_m/ϕ_0	ϕ_m[a]	*CMC*[b] (M)
PS-6	25	$(5{\cdot}9 \pm 0{\cdot}1) \times 10^{-4}$	$0{\cdot}067 \pm 0{\cdot}016$	0·027	*c.* 4×10^{-3} (25°C, [7])
PS-9	25	$(8{\cdot}6 \pm 0{\cdot}4) \times 10^{-5}$	$0{\cdot}069 \pm 0{\cdot}030$	0·024	*c.* 2×10^{-3} (25°C, [7])
PN-6	25	$(3{\cdot}8 \pm 0{\cdot}3) \times 10^{-4}$	$0{\cdot}63 \pm 0{\cdot}03$	0·28	4×10^{-4} (25°C, [7])
PN-9	25	—	—	—	9×10^{-5} (25°C, [7])
CS-8	25	$(2{\cdot}2 \pm 0{\cdot}5) \times 10^{-3}$	$0{\cdot}33 \pm 0{\cdot}18$	0·19	
CS-8	46	$(3{\cdot}2 \pm 1{\cdot}6) \times 10^{-3}$	$0{\cdot}36 \pm 0{\cdot}26$	0·21	*c.* 8×10^{-3} (45°C)[c]
CS-10	25	$(1{\cdot}0 \pm 0{\cdot}1) \times 10^{-3}$	$0{\cdot}11 \pm 0{\cdot}10$	0·064	
CS-10	46	$(1{\cdot}0 \pm 0{\cdot}2) \times 10^{-3}$	$0{\cdot}12 \pm 0{\cdot}10$	0·072	$2{\cdot}5 \times 10^{-3}$ (45°C, [6])

[a] Calculated using the ϕ_0 values given in Table 1. The fluorescence quantum yields of CS-8 and CS-10 were independent of temperature between 25 and 46°C.
[b] Determined from surface activity measurements using the du Nouy ring-detachment method. References are given in parentheses.
[c] L. A. Holt, personal communication.

are also included in Table 2. Replacement of the negatively charged sulphonate group in PS-6 by a quaternary ammonium group of opposite charge (PN-6) caused a small decrease in the CMC which may reflect the presence of the additional methylene hydrophobic group in the quaternary ammonium substituent. As noted above, the formation of micelles of PN-6 was accompanied by a relatively small decrease in the fluorescence quantum yield ($\phi_m/\phi_0 = 0{\cdot}63$), in contrast to the strong fluorescence quenching ($\phi_m/\phi_0 \sim 0{\cdot}07$) that was observed for the long-chain pyrazoline sulphonates. The mechanism of the micellar fluorescence quenching reaction is a matter for conjecture, but it may be inferred from the present results that the quaternary ammonium group hinders in some way the approach of excited and ground-state molecules in the outer region of the micelle where, presumably, the pyrazolyl head groups are located. There is evidence[17,18] that the π-electron ring systems of aromatic molecules interact weakly with quaternary ammonium head groups of surfactants, and it is believed that interactions of this type are responsible both for the greater solubility of aromatic molecules in cationic than in anionic surfactant micelles and for the tendency of aromatics to bind at the micelle–water interface. Similar interactions may occur in the head group region of the quaternary ammonium pyrazoline micelles, thereby affecting the efficiency of the self-quenching reaction.

The CMCs of the long-chain coumarin sulphonates are considerably higher than those of the long-chain pyrazoline sulphonates (see Table 2). The

measured values for CS-8 (2–3 × 10^{-3} M) and CS-10 (10^{-3} M) are close to the reported values[16] for sodium tetradecyl-1-sulphonate (2·2 × 10^{-3} M) and sodium hexadecyl-1-sulphonate (7 × 10^{-4} M), respectively, which implies that the coumarin ring system has an effective hydrocarbon chain length of about six carbon atoms.

Also included in Table 2 are the CMCs of the long-chain pyrazolines and coumarins determined[6,7] from surface activity measurements. The CMC value thus obtained for the cationic pyrazoline (PN-6) agrees well with the value derived from the fluorescence quenching data, but the values determined for the anionic surfactants are consistently higher than those obtained from fluorescence quenching. In the case of the pyrazoline sulphonates (PS-6 and PS-9) the two methods give very different CMC values. Aerial oxidation and low solubility at concentrations near the CMC reportedly[6] make surface activity measurements on these compounds imprecise. Although the CMC of a surfactant is often used as a measure of its surface activity, adsorption at the liquid–air interface and micellization can each respond very differently to structural changes in the surfactant molecule,[19] and it may be partly for this reason that the surface activity and fluorescence quenching results are not in accord.

3.3 Solubilization of spectroscopic probes

The ability to solubilize compounds that are otherwise insoluble in aqueous solution is an important property of micellar systems. The fluorescence probe approach[1–3] to the study of micellar properties relies on there being a change in some readily observable property of the probe molecule, such as its fluorescence quantum yield or lifetime, in the presence of micelles.

Many of the commonly used probes of membrane and micelle structure were found to be unsuitable for studying the micellization behaviour of the fluorescent surfactants because (1) the fluorescence of the probe molecule was completely masked by the intense fluorescence emitted by the surfactant itself or (2) the probe interacted strongly with the surfactant molecules, causing a marked change in its spectral properties. Two lipid probes that were solubilized by the micelle-forming coumarins without suffering these drawbacks were Nile Red (9-diethylamino-5H-benzo-[α]phenoxazine-5-one) and NBD-dioctylamine (4-[*N*,*N*-dioctyl]amino-7-nitrobenz-2-oxadiazole). Nile Red was solubilized to an appreciable extent by micellar solutions of CS-8 and CS-10, whereas NBD-dioctylamine was solubilized only by CS-10. Table 3 summarizes the spectral properties of Nile Red in several surfactant systems.

Nile Red is a strongly fluorescent molecule whose unique fluorochromic properties make it a useful lipid stain.[20,21] The fluorescence excitation and

TABLE 3
Spectral Characteristics of Nile Red in Various Aqueous Micellar Systems at 25°C

Surfactant (5×10^{-3} M)	λ_{max} (*ex*) (*nm*)	λ_{max} (*em*) (*nm*)	*Relative fluorescence intensity*[a]
Triton X-100	580	642	100
CTAC	588	638	95
SDS	593	646	2
SDS (0·05 M)	597	646	68
CS-8	601	646	28
CS-10	596	639	57
PS-6	—	—	<0·1
PS-9	—	—	<0·1
PN-6	570	605	0·2
PN-9	577	604	0·2

[a] The excitation and emission wavelengths were 540 and 640 nm, respectively. The concentration of Nile Red was $8{\cdot}5 \times 10^{-6}$ M.

emission maxima are extremely sensitive to the hydrophobicity of the solvent environment and vary from 484 and 529 nm in hydrocarbon solvents such as *n*-heptane to 559 and 629 nm in ethanol and 591 and 657 nm in water. The values that we obtained in ethanol (564 and 626 nm) differed only slightly from the published values, the variation being due probably to differences in the instrumental conditions used for measuring the spectra.

In general, the excitation and emission maxima of Nile Red in the various surfactant systems (Table 3) lie near the respective maxima in ethanol or water, indicating that the probe is located in a hydrophilic environment near the surface of the micelle. The relative fluorescence intensities of Nile Red in solutions of CS-8 and CS-10 are at least two orders of magnitude greater than those in solutions of the cationic pyrazolines (PN-6 and PN-9), which in turn are greater than those in solutions of the anionic pyrazolines (PS-6 and PS-9). Although the probe displayed small shifts in the spectral maxima which might be indicative of differences in surface polarity between the micellar systems, the interpretation of these shifts is made difficult by the likelihood of specific interactions, such as hydrogen bonding, which can alter[20] the spectral properties of the probe molecule.

The fluorescence of Nile Red in aqueous solutions containing CS-8 and CS-10 showed an abrupt increase in intensity as the surfactant concentration was increased from a value below the CMC to one above it (see Fig. 6). Extrapolation of the lines of best fit to the fluorescence data in the regions of high and low slope yielded values of $3{\cdot}9 \times 10^{-3}$ M and $1{\cdot}4 \times 10^{-3}$ M for the CMCs of CS-8 and CS-10, respectively, in water at

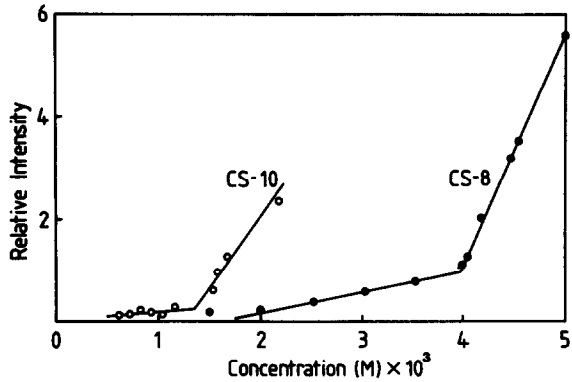

Fig. 6. Fluorescence intensity of Nile Red for varying concentrations of CS-8 and CS-10 in water at 46°C.

46°C. The results of the fluorescence probing experiment are significantly higher than those obtained from the fluorescence quenching data (see Table 2), indicating that the solubilized additive may have changed slightly the properties of the host micelle.

3.4 Determination of aggregation number

Another fundamental parameter of micelle-forming systems that is often investigated using fluorescence probe techniques is the micellar aggregation number.[1-3] The method that we have used is based[12] on the static quenching of a fluorescent donor, the tris-(2,2'-bipyridine)-ruthenium II complex cation ($Ru(bipy)_3^{2+}$), by the hydrophobic quencher, 9-methylanthracene. The merits of the technique and its application to micellar systems are well documented,[2,3,12,22] and will not be discussed here.

If the fluorescence of a micelle-associated donor is quenched (in the presence of completely micellized quencher, Q) solely by a static quenching process, then the ratio of the fluorescence intensities (I/I_0) in the presence of Q to that in the absence of Q is given by the expression:[12]

$$\ln(I_0/I) = [Q] \times \bar{n}/([\text{surfactant}] - \text{CMC}) \qquad (6)$$

where $\bar{n}$ is the mean aggregation number and [surfactant] refers to the macroscopic concentration of the surfactant. It is assumed in this analysis that the concentration of free surfactant monomer in equilibrium with micelles remains constant above the CMC.

Figure 7 shows the dependence of fluorescence intensity (solid circles) upon the concentration of CS-10, keeping the quencher concentration fixed at $2{\cdot}02 \times 10^{-5}$ M. The sample temperature was maintained at 50°C to overcome turbidity problems which were exacerbated by the presence of the

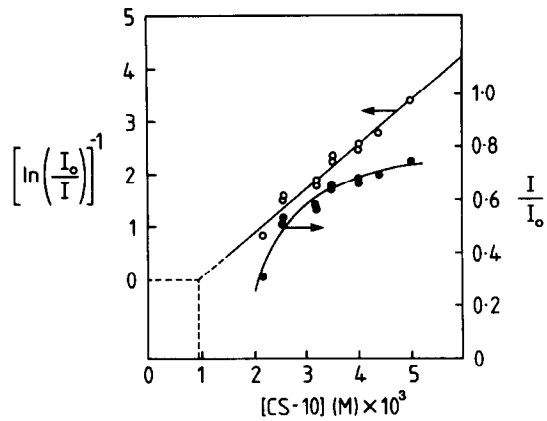

Fig. 7. Dependence of the $Ru(bipy)_3^{2+}$ fluorescence intensity (solid circles) upon the concentration of CS-10 at a fixed quencher (9-methylanthracene) concentration of $2{\cdot}02 \times 10^{-5}$ M (50°C). An analysis of the data according to eqn (6) is shown by the open circles. The excitation and emission wavelengths were 450 and 640 nm, respectively.

small amount of ethanol (0·5% by volume) that was used for the addition of quencher. The fluorescence intensity increased with increasing concentration of the surfactant, as predicted by theory. Figure 7 also shows (open circles) an analysis of the data according to eqn (6). The slope (837) of the line of best fit can be equated to $\{[Q].\bar{n}\}^{-1}$, from which we obtained a mean aggregation number $\bar{n} = 59 \pm 8$. The intercept of this line at the maximum quenching limit gave a value of $(9{\cdot}3 \pm 4{\cdot}7) \times 10^{-4}$ M for the CMC of CS-10 which agrees, within experimental error, with the value ($1{\cdot}0 \times 10^{-3}$ M) obtained by the fluorescence quenching method (see Table 2).

The mean aggregation number can also be derived from measurements of the fluorescence intensity of $Ru(bipy)_3^{2+}$ as a function of the concentration of quencher (Q) at a fixed surfactant concentration. Figure 8 shows a plot of

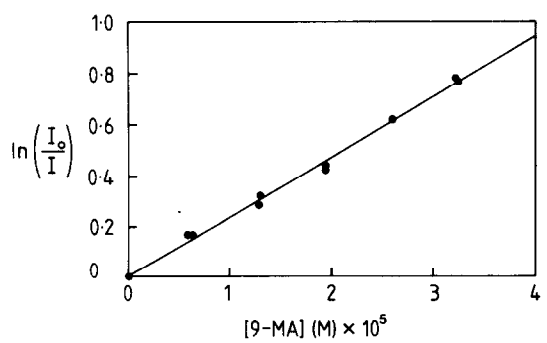

Fig. 8. Quenching of the fluorescence of $Ru(bipy)_3^{2+}$ by 9-methylanthracene at a fixed concentration ($3{\cdot}9 \times 10^{-3}$ M) of CS-10, plotted according to eqn (6). Other conditions as given in the caption to Fig. 7.

$\ln(I_0/I)$ vs $[Q]$ according to eqn (6), which yields a straight line passing through the origin with slope $\bar{n}/([\text{surfactant}] - \text{CMC})$. Using the CMC value ($1{\cdot}0 \times 10^{-3}$ M) obtained previously, we obtained (from three replicate determinations) a mean aggregation number $\bar{n} = 71 \pm 4$. The value of $\bar{n}$ obtained in this manner was consistently higher than the value ($\bar{n} = 59$) obtained from the $\{\ln(I_0/I)\}^{-1}$ vs [surfactant] plot (Fig. 7). Polydispersity in micelle size and variability in the micellar aggregation number at surfactant concentrations near the CMC[23] are possible reasons for the disparity. Given that the range over which the concentration of CS-10 could be varied was very limited (for solubility reasons), and that the degree of scatter in the experimental data obtained from the previous analysis (Fig. 7) was quite large, the higher value of $\bar{n}$ obtained at a fixed surfactant concentration (at a value well above the CMC to ensure proper micellization) is possibly the more reliable one.

Attempts to determine the micellar aggregation numbers of the other fluorescent surfactants were unsuccessful. Fluorescence quenching was not observed for micellar solutions of the quaternary ammonium pyrazolines, indicating a lack of solubilization of one or other (or both) of the components of the donor/acceptor pair. The fluorescence of $Ru(bipy)_3^{2+}$ was strongly quenched in the presence of the long-chain pyrazoline sulphonates, thus making it unsuitable as a fluorescent donor for these systems. Quenching of the $Ru(bipy)_3^{2+}$ fluorescence by 9-methylanthracene was observed in concentrated solutions of CS-8, but the range of concentrations (above the CMC) that were amenable to study was too restricted to permit the technique to be applied with any degree of reliability to this compound.

4 CONCLUSION

The aim of this work was to characterize the spectral properties of a range of fluorescent alkaryl-2-pyrazolines and 3-alkyl-7-hydroxycoumarins containing *n*-alkyl substituents of varying chain length, and to investigate the self-association behaviour of these compounds in water.

Plots of the fluorescence quantum yield against concentration for the higher members of each series showed a sharp break at a well-defined concentration, in contrast to the smoothly decreasing curve that was characteristic of the lower members of the series. The discontinuity is interpreted as evidence of micelle formation, and the concentration at which it occurs as the CMC of the fluorescent surfactant in question. From the CMC values thus obtained, we conclude that the pyrazoline and coumarin ring systems have an effective straight hydrocarbon chain length of about ten and six carbon atoms respectively. Anionic pyrazoline and coumarin

sulphonates showed strong self-quenching of their fluorescence at concentrations above the CMC, whereas the fluorescence of cationic (quaternary ammonium) pyrazolines was affected only slightly by changes in concentration. The occurrence of a specific interaction between the quaternary ammonium group and the π-electron ring system of the pyrazoline moiety is suggested as a possible reason for this difference.

Two lipid probes, Nile Red and NBD-dioctylamine, were solubilized by long-chain coumarin surfactants, resulting in a strong enhancement of their fluorescence. Neither probe was solubilized to an appreciable extent by the pyrazoline surfactants. CMC values determined using Nile Red as a fluorescent probe were slightly higher than the values obtained from studies of the self-quenching of the surfactant fluorescence.

The micellar aggregation number ($\bar{n}$) of the highest member of the coumarin series was determined from fluorescence quenching experiments employing $Ru(bipy)_3^{2+}$ and 9-methylanthracene as the donor/quencher pair. The values obtained ranged from $\bar{n} = 59$ to $\bar{n} = 71$ according to the method of analysis used.

REFERENCES

1. Singer, L. A., in *Solution Behavior of Surfactants. Theoretical and Applied Aspects*, Vol. 1, ed. K. L. Mittal & E. J. Fendler, Plenum Press, New York, 1982, p. 73.
2. Turro, N. J., Grätzel, M. & Braun, A. M., *Angew. Chem. Int. Ed. Engl.*, **19** (1980) 675.
3. Zana, R., *Surfactant Solutions. New Methods of Investigation*, Ch. 5, Marcel Dekker, New York, 1987.
4. Turro, N. J., Tanimoto, Y. & Gabor, G., *Photochem. Photobiol.*, **31** (1980) 527.
5. Shore, N. E. & Turro, N. J., *J. Am. Chem. Soc.*, **97** (1975) 2488.
6. Holt, L. A. & Stapleton, I. W., *J. Soc. Dyers Colour*, **104** (1988) 387.
7. Holt, L. A. & Stapleton, I. W., *Proc. Text. Inst. 1988 Annual World Conf. (Sydney)*, 10–13 July 1988, p. 420.
8. Stedman, E., *J. Chem. Soc.* (1927) 1902.
9. *Organic Syntheses, Collective Vol. I*, ed. H. Gilman & A. H. Blatt. John Wiley, New York, 1948, p. 442.
10. Melhuish, W. H., *J. Phys. Chem.*, **65** (1961) 229.
11. Leaver, I. H., *Aust. J. Chem.*, **32** (1979) 1961.
12. Turro, N. J. & Yekta, A., *J. Am. Chem. Soc.*, **100** (1978) 5951.
13. Zinsli, P. E., *J. Photochem.*, **3** (1974) 55.
14. Guilford, J. H., Jackson, W. R., Kanoktanaporn, S. & Bergmark, W. M., *Photochem. Photobiol.*, **42** (1985) 477.
15. Infelta, P. P. & Grätzel, M., *J. Chem. Phys.*, **70** (1979) 179.
16. Rosen, M. J., *Surfactants and Interfacial Phenomena*, Ch. 3. Wiley–Interscience, New York, 1978.

17. Almgren, M., Grieser, F. & Thomas, J. K., *J. Am. Chem. Soc.*, **101** (1979) 279.
18. Mukerjee, P. & Cardinal, J. R., *J. Phys. Chem.*, **82** (1978) 1620.
19. Rosen, M. J., in *Solution Chemistry of Surfactants*, Vol. 1, ed. K. L. Mittal. Plenum Press, New York, 1979, p. 45.
20. Greenspan, P. & Fowler, S. D., *J. Lipid Res.*, **26** (1985) 781.
21. Greenspan, P., Mayer, E. P. & Fowler, S. D., *J. Cell Biol.*, **100** (1985) 965.
22. Malliaris, A., *Adv. Colloid. Interface Sci.*, **27** (1987) 153.
23. Löfroth, J.-E. & Almgren, M., in *Surfactants in Solution*, Vol. 1, ed. K. L. Mittal & B. Lindman. Plenum Press, New York, 1984, p. 627.